High Resolution E-Jet Printed Temperature Sensor on Artificial Skin

T. Vuorinen[1], M.-M. Laurila[1], R. Mangayil[2], M. Karp[2] & M. Mäntysalo[1]

[1] Tampere University of Technology, Faculty of Computing and Electrical Engineering, Tampere, Finland
[2] Tampere University of Technology, Faculty of Natural Sciences, Tampere, Finland

Abstract—**Skin-conformable electronics research field has grown rapidly during the recent years. Body monitoring systems are shrinking in size and integrating more seamlessly with the human skin. To make these monitoring systems feasible options, new suitable materials and manufacturing processes needs to be studied. This paper presents materials and a simple fabrication process for skin-conformable, E-jet printed silver temperature sensors. Utilizing printing processes and biodegradable substrate materials, the skin-conformable electronics may become attractive for disposable systems by decreasing the manufacturing costs and reducing the amount of waste materials. In this study, the temperature sensors are fabricated with E-jet printed silver nanoparticle ink and the printing is done on a bacterial nanocellulose substrate. During the characterization, the silver temperature sensors were able reach more than 0.06 % per degree Celsius sensitivity and they exhibited positive temperature dependence.**

Keywords— **E-jet, printed electronics, temperature sensor, bacterial nanocellulose**

I. Introduction

One development direction in vital sign monitoring is to make the monitoring devices as user friendly as possible. The progress is done by shrinking the device dimensions, especially thickness, which helps the devices to integrate seamlessly with a human body. This requires wireless monitoring systems and new kind of device structures, such as skin-like electronics. Skin-conformable structures, that measure for example ECG [1][2], chronic wounds [3], and temperature [4–6], have already being studied with plastic substrates and the next step is to make the substrate material to integrate with the skin even more seamlessly. This can be done, for instance, by using temporary tattoo type of a materials to attach the electronics to the skin. In addition, to reduce the environmental impact in disposable systems, other materials than synthetic polymers need to be studied.

Cellulose, obtained from plants, is the most abundant biopolymer on Earth and is the biomaterial of choice for various industrial applications, for example, textile, pulp and paper [7]. However, the process of harvesting the cellulose content from lignocellulose requires harsh pretreatment steps with high-energy input and often generates byproducts (aromatic lignin derivatives) and/or toxic sulfoxide residues [7][8]. In addition to plants, production of extracellular cellulose in some bacterial genera has also been established [9–11]. Cellulose synthesized by microorganisms is highly pure (devoid of lignin and hemicellulose impurities) compared to plant-based cellulose. Thus, bacterial nanocellulose aids to circumvent the harsh processing step, making the production process sustainable. In terms of biopolymer characteristics, bacterial nanocellulose has high level of crystallinity, superior structural integrity, mechanical, optical, biodegradable and water holding properties [7].

In addition to suitable substrate materials, the skin-conformable electronics requires the functionalities found from a human skin. To match the receptor density in the skin, the manufacturing methods need to be able to fabricate very high resolution sensor structures for skin-conformable electronics. One option is to use electrohydrodynamic inkjet (E-jet) printing [12]. Compared to the conventional piezo or thermal actuator based inkjet devices, the E-jet offers up to ten times higher resolution and thousand fold ink viscosity range (10-20 mPa·s [13] vs 0.1-10000 mPa·s [14]. This enables the continued device miniaturization in the field of printed electronics, while still using the same low temperature inks developed for conventional inkjet devices.

In this paper, we report a manufacturing process and materials for high resolution E-jet printed silver temperature sensors. The sensors were fabricated using screen-printed, stretchable silver flake ink, E-jet printed silver nanoparticle ink, and bacterial nanocellulose substrate material. Sensors were characterized in ambient atmosphere to verify the temperature coefficient of resistance (TCR) of the printed sensors. Both the inks and the substrate material enable the printing fabrication of disposable, skin-conformable systems.

II. Materials and Methods

A. Bacterial nanocellulose cultivation

The bacterial nanocellulose films were prepared from *Komagataeibacter xylinus*, a natural cellulose producer. To prepare the seed cultures for bacterial nanocellulose production, *K. xylinus* (from glycerol stocks) were inoculated into 5 ml glucose (20 g L^{-1}) amended buffered Hestrin-Schramm (HS, pH 6.0) growth medium [g L^{-1}: peptone, 5; yeast extract, 5; di-sodium hydrogen phosphate, 2.7 and citric acid, 1.15) and

grown at 30°C/180 rpm for 4 days. For bacterial nanocellulose production, the seeds cultures were inoculated to 30 ml of similar growth medium in sterile petri dish and incubated statically at 30°C for 4 days.

At the end of the cultivation, bacterial cells entrapped within the produced cellulose were inactivated by rinsing the nanocellulose sheets with ultrapure water (Milli-Q, EMD Millipore, Germany) and incubating overnight in 0.5 M sodium hydroxide solution at 60˚C. The alkali solution was removed by repeated washing with ultrapure water until neutral pH was attained. Subsequently, the washed bacterial nanocellulose sheets were dried at 60˚C for 16 hours and the dried nanocellulose films were used in this study.

B. Substrate preparation and screen printing process

The nanosellulose films are too thin to be used in the printing process without a carrier. To make the carrier, a 125 µm thick Melinex ST506 polyethylene terephthalate (PET) films were coated with a layer of Sylgard 184 polydimethylsiloxane (PDMS). A layer of PDMS, with 200 µm wet thickness, was spread using a CX202 bar coater together with an applicator. The coating speed was 18 mm/s, and the coated samples were cured in a convection oven at 130°C for 10 minutes. The PET film provides mechanical support and the PDMS functions as a release layer, so that the nanocellulose could be removed from the carrier without softening the cellulose with water.

Silver conductors were screen printed using TIC SCF-300 screen printer and CI-4040 stretchable Ag/AgCl ink (ECM). The silver ink contains 40 – 50 wt% silver powder and 5 – 15 wt% silver chloride powder diluted in a diethylene glycol ethyl ether acetate solvent. The printed pattern was defined by a polyester screen with a mesh count of 79 threads cm^{-1}, a mesh opening of 69 µm, and a stretching angle of 22.5°. After printing, the silver patterns were annealed in a convection oven at 130 °C for 30 minutes.

C. High resolution inkjet printing process

The meander sensor structures were fabricated using a commercially available E-jet device, Super Inkjet (Super Inkjet Technology Inc., Japan). In the current application, the sensors are printed using DGP 40TE-20C silver nanoparticle ink (Advanced Nano Products Ltd, Korea). The ink had a solid content of 30 – 35 wt% diluted in triethylene glycol monoethyl solvent [15]. After printing the ink was sintered at 150 °C for 1 h.

The operation of E-jet is based on electric field generated droplet emission from ink meniscus at the tip of a glass nozzle. The size of the droplets can be controlled by adjusting the field intensity between the meniscus and grounded xy-stage i.e. by changing the DC-, or peak voltage (V_{DC}, V_{peak}) and nozzle-to-substrate distance (d). The conductor width is further controlled by the relationship between droplet ejection frequency (f) and printing speed (v), while the conductor thickness is principally controlled by the number of printed layers. The printing parameters are presented in Table 1.

Table 1. E-Jet print parameters for meander structure

Parameter	Value
V_{DC} (V)	0
V_{peak} (V)	440
f (Hz)	10
v (µm/s)	130
d (µm)	20
number of layers	20

The print was performed in ambient atmosphere with recorded temperature of 21.1°C and relative humidity of 20 %.

D. Electrical characterization setup

A resistance measurement setup was used, together with a heating/cooling unit, to assess the resistance dependence on

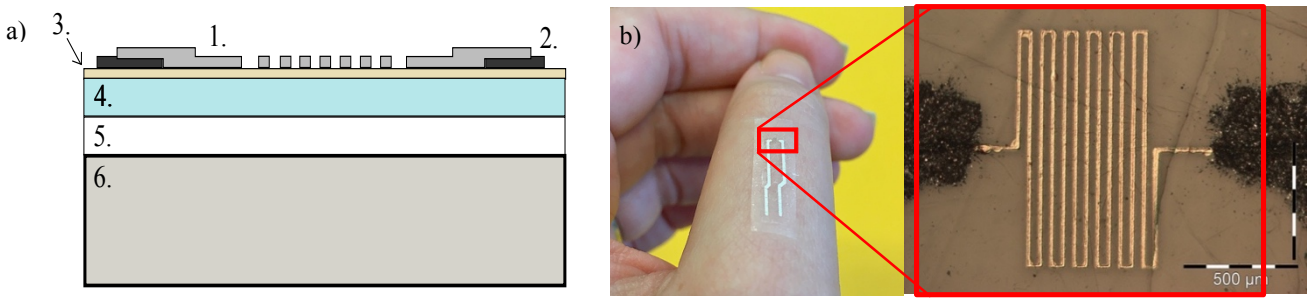

Fig. 1 A) Cross section of the sample on the Peltier element. B) A photograph and an optical microscope image of the silver temperature sensor.

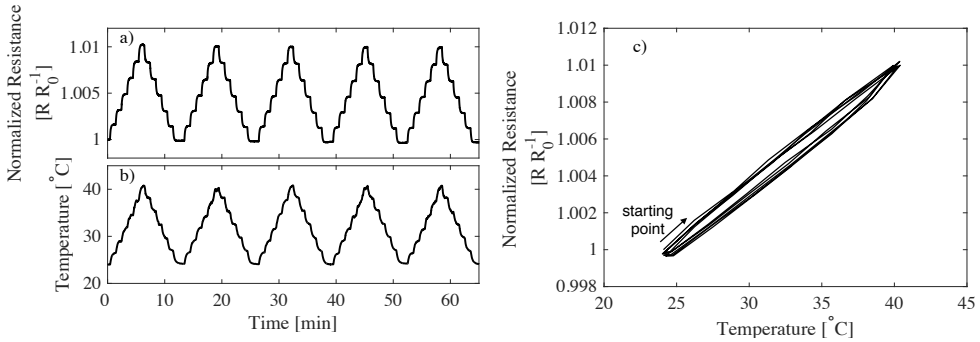

Fig. 2 a) normalized resistance and b) measured temperature from the samples. Temperature was increased and decreased between 24 °C and 41 °C during the measurements and this cycling was done five times for the samples. The measured data from a) and b) is presented in form of normalized resistance as a function of temperature c) during the five temperature cycles between 24 °C to 41 °C.

temperature in ambient conditions. In the resistance measurement setup, a LabVIEW system design software driven digital multimeter in a VirtualBench (National Instruments) measured the resistance of the samples with a 1 Hz sampling rate. VirtualBench also drove the heating/cooling unit, which consisted of a Peltier element and Silverstone Tundra TD03 liquid cooler that kept one side of the Peltier at a constant room temperature. TC-08 thermocouple Data Logger (Pico Technology) was used to measure the temperature of the plaster surface. During the electrical characterization, VirtualBench increased and decreased the Peltier voltage stepwise using 0.4 V steps and the voltage was kept constant for 1 min. The temperature cycling fluctuated approximately between 24 °C and 41 °C, and complete cycles (increase from 24 °C to 41 °C and decrease form 41 °C to 24 °C) were done five times for the samples.

III. Results

Fig. 1 a) shows the multilayered structure of the samples. E-jet printed silver nanoparticle sensor (1.) is fabricated on top of the screen-printed silver conductors (2.). Nanocellulose substrate (3.) is spread on the PDMS release layer (4.). PET film (5.) provides mechanical support during the processing steps and measurements. The sample is placed on a Peltier element (6.) in the electrical characterization setup. Fig. 1 b) presents a photograph of the sample being attached to the skin and an optical microscope image of the E-jet printed sensor part. The meander shaped sensor had approximately 20 µm conductor width with 50 µm spacing.

The temperature cycling was repeated five times for the samples and results from one sample is presented in Fig. 2. Fig. 2 a) shows the results as normalized resistance and (b) corresponding temperature values. In Fig. 2 c) the measured data from a) and b) is transformed in form of normalized resistance as a function of temperature during the five temperature cycles.

Fig. 3 presents a response time and a recovery time for one sample. In Fig. 3 (left side) the input voltage of the Peltier element is increased by 0.4 V and is then kept unaltered for 1 minute. The 90th percentile response time was 15 seconds with this Peltier element setup. It needs to be noticed that the Peltier element also has a response time which reflects to the response time of the temperature sensor. Fig. 3 (right side) shows a 90th percentile recovery time of 17 seconds for the sensor when the Peltier voltage is decreased by 0.4 V.

IV. Discussion

Dielectric substrates, such as nanocellulose, pose additional challenges for E-jet printing process since the remaining charge in printed droplets takes longer to decay and may therefore affect the droplet generation during printing of subsequent layers. One approach to compensate for this effect is to print alternately positive and negative droplets (i.e. by setting V_{DC} to 0 Volts) [16]. The spraying of droplets on dielectric surfaces can be minimized by reducing the nozzle-to-substrate distance and print frequency. As a trade-of, the printing speed must be reduced which will limit the throughput of the process. Taking these restrictions in the account, the print parameters were calibrated to produce approximately 20 µm conductor width (Table 1).

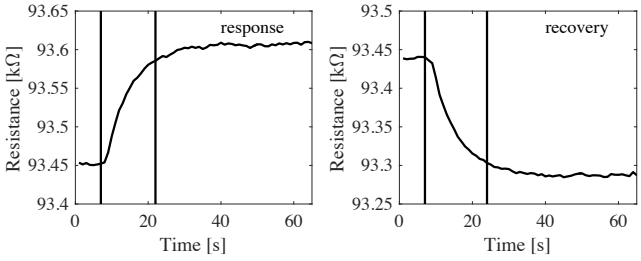

Fig. 3 *One heating step and one cooling step to visualize the response time and the recovery time. The 90th percentile response time was 15 seconds and the 90th percentile recovery time was 17 seconds.*

During the temperature cycling the resistance was increasing when the temperature was increasing, as was expected from the silver sensor since the silver is a positive temperature coefficient (PTC) material. The level of hysteresis stays low and the TCR is 0,0602 % per degree Celsius. The sensor would not compete in efficiency with already existing temperature sensors but the sensor could be used in its present form to indicate if the local body temperature is going up or down. This can be a beneficial indicator of fever or healing infections.

V. Conclusions

The fabrication process presented in this paper, enable a straightforward fabrication procedure for E-jet printed silver temperature sensors compatible with skin-conformable bacterial nanocellulose substrate. Ideally the printed skin-like sensors are targeted for disposable systems. This is due to the decreased number of fabrication steps, reduced amount of waste material and possibility to use new kind of substrate materials, compared to the traditional lithography processed devices. Using bacterial nanocellulose as the substrate material minimizes the negative environmental impact remarkably compared to plastic substrates.

The sensors were fabricated with E-jet printed nanoparticle silver ink and screen printed silver fake ink on top of a skin-formable nanocellulose substrate, which provides temporary-tattoo type of base for the system. The completed printed system is light-weight, thin, and can seamlessly integrate with the skin. The device has the possibility to monitor temperature changes directly on human skin with a TCR value 0.06% per degree Celsius in ambient conditions.

Acknowledgment

This work was funded by the Academy of Finland (grant no. 288945 and 294119). T. Vuorinen would like to thank KAUTE-säätiö and Tekniikan edistämissäätiö for personal financial support.

Conflict of Interest

The authors declare that they have no conflict of interest.

References

1. Vuorinen T, Vehkaoja A, Jeyhani V, et al (2016) Printed, skin-mounted hybrid system for ECG measurements. 2016 6th Electron Syst Technol Conf 1–6. doi: 10.1109/ESTC.2016.7764710
2. Khan Y, Garg M, Gui Q, et al (2016) Flexible Hybrid Electronics: Direct Interfacing of Soft and Hard Electronics for Wearable Health Monitoring. Adv Funct Mater 26:8764–8775. doi: 10.1002/adfm.201603763
3. Farooqui MF, Shamim A (2016) Inkjet printed wireless smart bandage. 2016 IEEE Middle East Conf Antennas Propag 1–2. doi: 10.1109/MECAP.2016.7790102
4. Hong SY, Lee YH, Park H, et al (2016) Stretchable Active Matrix Temperature Sensor Array of Polyaniline Nanofibers for Electronic Skin. Adv Mater 28:930–5. doi: 10.1002/adma.201504659
5. Bali C, Brandlmaier A, Ganster A, et al (2016) Fully Inkjet-Printed Flexible Temperature Sensors Based on Carbon and PEDOT:PSS1. Mater Today Proc 3:739–745. doi: 10.1016/j.matpr.2016.02.005
6. Vuorinen T, Niittynen J, Kankkunen T, et al (2016) Inkjet-printed graphene/PEDOT:PSS temperature sensors on a skin-conformable polyurethane substrate. Sci Rep. doi: 10.1038/srep35289
7. Jozala AF, de Lencastre-Novaes LC, Lopes AM, et al (2016) Bacterial nanocellulose production and application: a 10-year overview. Appl Microbiol Biotechnol 100:2063–2072. doi: 10.1007/s00253-015-7243-4
8. Lee K-Y, Buldum G, Mantalaris A, Bismarck A (2014) More Than Meets the Eye in Bacterial Cellulose: Biosynthesis, Bioprocessing, and Applications in Advanced Fiber Composites. Macromol Biosci 14:10–32. doi: 10.1002/mabi.201300298
9. Schramm M, Hestrin S (1954) Factors affecting production of cellulose at the air/liquid interface of a culture of Acetobacter xylinum. J Gen Microbiol 11:123–129. doi: 10.1099/00221287-11-1-123
10. Hungund BS, Gupta SG (2010) Production of bacterial cellulose from Enterobacter amnigenus GH-1 isolated from rotten apple. World J Microbiol Biotechnol 26:1823–1828. doi: 10.1007/s11274-010-0363-1
11. Tanskul S, Amornthatree K, Jaturonlak N (2013) A new cellulose-producing bacterium, Rhodococcus sp. MI 2: Screening and optimization of culture conditions. Carbohydr Polym 92:421–428. doi: 10.1016/j.carbpol.2012.09.017
12. Laurila MM, Khorramdel B, Mäntysalo M (2017) Combination of E-Jet and Inkjet Printing for Additive Fabrication of Multilayer High-Density RDL of Silicon Interposer. IEEE Trans Electron Devices 64:1217–1224. doi: 10.1109/TED.2016.2644728
13. Hutchings IM, Martin GD (2012) Introduction to Inkjet Printing for Manufacturing. In: Inkjet Technol. Digit. Fabr. John Wiley & Sons, Ltd, pp 1–20
14. Murata K, Masuda K (2011) Super Inkjet Printer Technology and Its Properties. Convert e-Print 108–111.
15. Advanced Nano Products Ltd. ANP Silverjet datasheet at:http://anapro.com/eng/product/silver_inkjet_ink.html.
16. Wei C, Qin H, Ramírez-Iglesias NA, et al (2014) High-resolution ac-pulse modulated electrohydrodynamic jet printing on highly insulating substrates. J Micromech Microeng 24:45010.

Enter the information of the corresponding author:

Author: Tiina Vuorinen
Institute: Tampere University of Technology
Street: Korkeakoulunkatu 3
City: Tampere
Country: Finland
Email: tiina.vuorinen@tut.fi